

5 Regional Element Distribution Patterns and the Problem of Pregranitic Tin Enrichments

5.1 General

The petrological stratification of the lithosphere implies a priori a vertical geochemical stratification on a global scale. Besides this general situation, the existence of metal provinces is often seen from a transformistic point of view as being related to geochemical anomalies of regional extent (Routhier 1980; Schuiling 1967; etc.). Such anomalies should be traceable both by indirect methods such as element evolution trends in granitic differentiation suites as attempted above, and by direct geochemical sampling on a regional scale. Igneous rocks of different origin can be used as probes into their crustal or mantle source regions, high crustal levels can be studied by systematic sampling of outcrops of different lithological units. Such studies need, however, a clear distinction between the regional reference system not affected by hydrothermal alteration and those portions which are hydrothermally overprinted. A metallogenic province of hydrothermal ore deposits contains by definition large-scale hydrothermal haloes, the size of which is sometimes underestimated. Geochemical haloes around hydrothermal tin ore deposits are commonly several km wide (e.g. Grant et al. 1977; Lehmann 1985; Polya 1988). A mix-up of genetically different sample populations must lead to wrong conclusions.

The literature gives numerous indications of regional metal anomalies (anomalous element contents compared to equivalent rock types elsewhere). Pre-granitic, sedimentary tin and tungsten enrichments have been repeatedly reported from tin and tin-tungsten districts in the eastern USSR and southern China. These data are, however, poorly documented and unverifiable. The problem with such studies is evident from the example of the Erzgebirge.

5.2 Erzgebirge, Germany, and Iżera Mountains, Poland

The Proterozoic basement of the Erzgebirge includes a few km northwest of Freiberg a blastomylonitic rock unit with stratabound impregnations of pyrite, known as Felsithorizont. Exploration work in the 1960's established that

subeconomic tin contents occur in this rock unit over a strike length of about 10 km. The Felsithorizont of Freiberg-Halsbrücke consists of a heterogeneous sequence of mafic to silica-rich volcanics and of clastic and calcareous sediments, affected by polymetamorphism up to amphibolite grade. Baumann and Weinhold (1963), Baumann (1965) and Weinhold (1977) interpreted the associated tin mineralization as of syngenetic, submarine, hydrothermal-sedimentary formation, which thereby was claimed to be of Proterozoic age with only minor transformation during the Hercynian granite magmatism. This diagnosis of general metallogenetic importance must, however, be rejected in the light of more recent investigations (Kormilicyn 1987; Lorenz and Schirn 1987; Richter 1987).

Systematic studies during the last years demonstrate that the Felsithorizont is a heavily mylonitized sequence of about 1000 m thickness, in which the regional medium-grade metamorphism is reequilibrated to greenschist-facies mineral associations in the most permeable rock portions. Tin mineralization in the form of disseminations is located in metasomatically transformed rock portions; cassiterite-bearing veinlets occur in competent rock units. The general ore assemblage of cassiterite, quartz, pyrite (chalcopyrite and other sulphides are much less abundant), carbonates and fluorite corresponds to the chlorite-sulphide zone of other epigenetic tin deposits of Hercynian age of the Erzgebirge. K-Ar age dating on the retrograde-hydrothermal, chlorite-dominated and mineralized rock portions gave an age of 275 Ma, whereas the non-altered and unmineralized rock portions gave the age of the regional metamorphism of 430 Ma. The unaltered portions of the Felsithorizont have no anomalous tin contents; the contention by Plimer (1980:279) of a "high Sn content of the mafic volcanics of the Erzgebirge" has no basis. A detailed account of this misunderstanding is given by Lorenz and Schirn (1987).

A similar situation seems to apply to strata-bound tin occurrences about 150 km further east in the Karkonosze-Izera Massif at the Czech-Polish border (Fig. 72). There, around the village of Gierczyn, a Proterozoic rock unit about 800 m thick and with a lateral extent of about 35 km is locally associated with tin, copper and cobalt mineralization which was mined in the 16th to 18th century. The ore-bearing horizon (in the German literature known as "zinnerzführendes Fahlband"; Buch 1802; Petrascheck 1933; Putzer 1940, 1942) consists of garnet-mica schist with zones of retrograde chloritization. Mineralization occurs as impregnations and in quartz veinlets in such chloritized zones and consists of cassiterite in association with a polymetallic sulphide assemblage dominated by pyrrhotite, with locally abundant Ni and Co sulphides. The ore-bearing sequence is underlain by the shallow intrusion of the Hercynian Karkonosze granite (around 300 Ma old), which is exposed

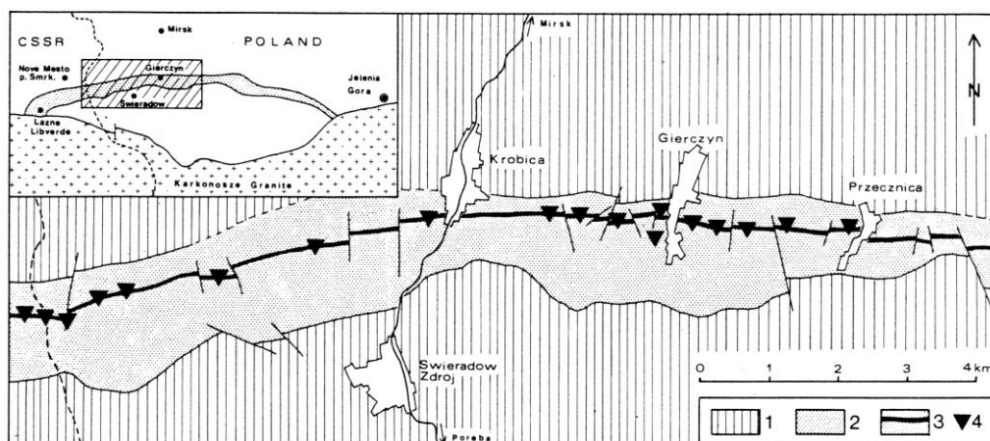


Fig. 72. Generalized geological map of the Gierczyn area, Izera Mountains, Poland. (Lehmann and Schneider 1981:748). 1 augen and flaser gneiss (meta-greywacke); 2 chlorite-mica-quartz schist (+garnet, kyanite, chloritoid); 3 garnet-mica schist (+amphibole); 4 ancient mines (Sn-Cu-Co mineralization)

10 km to the south and which encloses and cuts the ore horizon in a crescent-shaped form (Fig. 72). The Karkonosze granite is host to small tin occurrences in greisen zones (Kozłowski and Karwowski 1975; Kozłowski et al. 1975).

The source material of the garnet-mica schist was a clay-silt-limestone sequence which was transformed by both regional and thermal metamorphism. Volcanic influence is not documented. The conventional concept of a genetic relationship of the stratabound tin mineralization with the neighbouring Karkonosze granite (Berg 1922; Petrascheck 1933; Putzer 1940) was dismissed by Jaskolski (1960, 1962) and Szalamacha and Szalamacha (1974) on the basis of textural-geometric relationships, reviving the conclusions of Buch (1802) from the earliest geological reconnaissance in this area. More recent studies are animated by successful tin exploration in the Gierczyn area and are in favour of a granitic source of the tin mineralization (Kozłowski 1978; Speczik and Wiszniewska 1984). Petrographic and fluid inclusion data define large-scale hydrothermal-metasomatic overprint patterns which have been dated radiometrically with 320-300 Ma (Speczik and Wiszniewska 1984).

Pälchen et al. (1987) calculated regional Clarke values for the pre-granitic basement of the Erzgebirge. These data are summarized in Table 5 and are

Table 5. Regional Clarke values and regional element abundances in lithostratigraphic units of the pre-Hercynian Erzgebirge (major elements in wt%, trace elements in ppm). Data from Pälchen et al. (1987). Global upper crustal references values from Taylor and McLennan (1985)

	1	2	3	4	5	6	7	8	9
Si	31.7	29.4	28.6	22.3	40.9	35.0	33.8	30.9	30.8
Al	8.2	10.6	10.9	8.2	3.8	7.0	7.7	9.0	8.0
Fe	3.58	5.07	5.29	8.96	1.83	1.94	1.95	4.22	3.50
Mg	1.09	1.13	1.17	5.6	0.24	0.27	0.43	1.16	1.33
Ca	1.23	0.52	0.14	6.4	0.14	0.46	0.76	0.89	3.00
Na	2.18	0.72	0.70	2.00	0.15	1.93	2.19	1.42	2.89
K	3.05	3.31	3.26	0.42	1.41	3.74	3.40	2.99	2.80
B	13	34	65	<10	46	12	15	32	15
Ba	660	515	675	80	355	160	490	565	550
Be	2.9	2.3	3.0	1.0	1.0	2.0	1.9	2.4	3.0
Co	11	11	14	49	5.3	2.0	2.7	11	10
Cr	48	65	72	240	21	24	18	60	35
Cu	25	26	26	60	14	9.0	9.3	26	25
F	610	625	765	450	210	600	685	615	720
Li	66	53	84	35	28	30	46	62	20
Mn	460	485	1050	1450	155	160	205	575	600
Ni	20	23	39	72	13	4.0	6.0	26	20
Pb	24	23	21	8	16	30	25	22	20
Rb	115	120	200	30	64	230	220	140	112
Sn	3.9	3.7	5.0	4.0	2.0	8.0	5.9	4.6	5.5
Sr	175	85	89	200	34	35	68	115	350
Ti	4150	4750	5600	11500	4050	1000	1500	4500	3000
V	68	91	115	300	29	12	18	80	60
W	1.8	1.6	1.9	1.0	1.0	3.5	4.2	2.4	2.0
Zn	80	77	115	90	30	40	55	83	71
Zr	205	240	160	110	730	60	105	195	190

1 = Paragneiss (n=32)

2 = Mica schist (n=25)

3 = Phyllite (n=353)

4 = Meta-basite (n=22)

5 = Quartzite (n=91)

6 = Meta-rhyolite ("Graugneis") (n=55)

7 = Meta-granitoid (n=197)

8 = Regional Clarke of pre-Hercynian Erzgebirge

9 = Clarke according to Taylor and McLennan (1985)

derived from a large number of representative rock samples which were carefully examined for absence of any signs of hydrothermal overprint. The average element contents of tin and tungsten, as well as of most other elements are very close to global averages for the upper crust. There is no indication for a pre-Hercynian tin enrichment such as a regional geochemical tin anomaly in the Erzgebirge basement.

This result contrasts with an earlier attempt by Weinhold (1977) to define regional element abundances in the metamorphic basement of the Erzgebirge. This study arrived at an arithmetic mean of 68 ppm Sn, based on 1725 rock samples. Numerous hydrothermally altered samples were, however, included in this calculation, which could have easily been identified by analysis of the frequency distribution of the data. The data evaluation by Weinhold (1977) is considered today as erroneous (see discussion in Pälchen et al. 1987) and illustrates the fact that any investigation on regional element abundances needs careful sample selection and verifiable data processing.

5.3 The Bolivian Tin Belt

The enormous boron and tin accumulations in the hydrothermal systems of the Bolivian tin belt could be derived from sedimentary tin and boron anomalies in the thick Lower Paleozoic sequences of that region, remobilized by hydrothermal convection cells associated with the Triassic and Tertiary magmatism (Petersen 1979). The country rock of both Triassic tin granites and Tertiary tin porphyries consists of a Lower Ordovician to Upper Devonian clastic sequence (shale, meta-sandstone and siltstone), with more than 10,000 m of stratigraphic thickness. This sequence is the result of intracratonic, marine sedimentation with source regions dominantly to the west of the shallow basin in the "Altiplano Massif" (Isaacson 1975), and has been folded and metamorphosed under very-low- to low-grade conditions during the Hercynian orogeny (Martinez 1980).

The Lower Paleozoic sequence has been sampled in a cross-section between La Paz and Coroico, about 50 km long and perpendicular to the strike of the eastern Andes (Lehmann et al. 1988). The 120 samples (1-2 kg each) from Middle Ordovician to Upper Silurian shales and meta-sandstones give mean values of tin and boron contents which correspond to averages of equivalent rock types from other parts of the world (Fig. 73). These data do not support the assumption of a regional tin or boron anomaly in the Lower Paleozoic

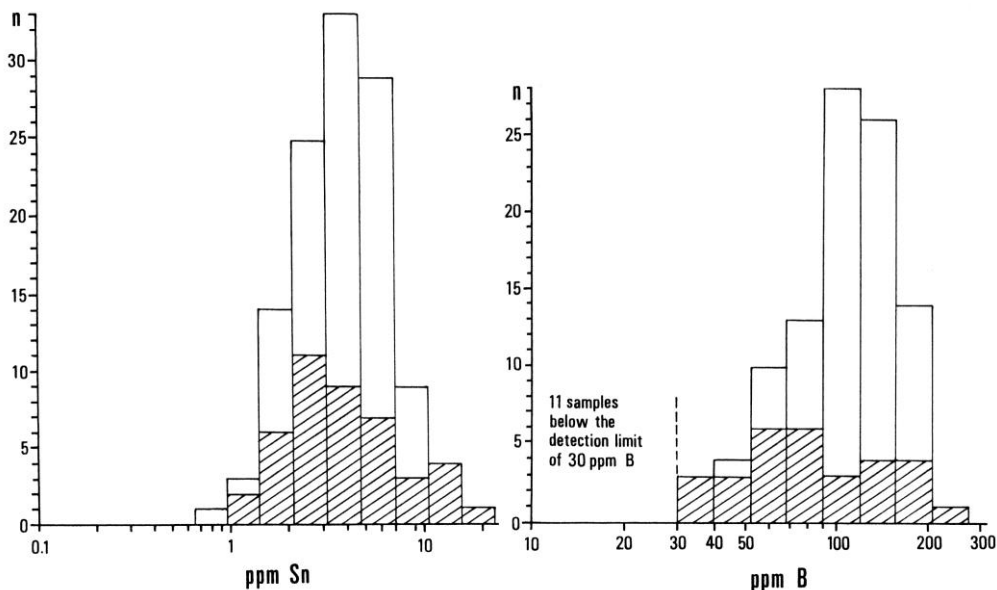


Fig. 73. Regional tin and boron abundances in the Ordovician-Silurian shale-sandstone sequence of the Cordillera Real, Bolivia. Sample section La Paz-Coroico; 110 rock samples. (Lehmann et al. 1988). Ruled: meta-sandstone; open boxes: shale. Eleven samples with <30 ppm B are meta-sandstones

sequence of the Bolivian tin belt. However, there is still the possibility that hypothetical pre-Hercynian tin and boron accumulations may be unexposed or may have gone undetected.

Lead isotope data on galena from some Bolivian tin deposits indicate an origin predominantly from crustal sources (Tilton et al. 1981). A discrimination between Paleozoic wall rocks or granitic intrusions and their Precambrian source material is, however, not possible.

Although the available geochemical data make a geochemical tin anomaly in the Paleozoic wall rocks of the tin-bearing igneous intrusions unlikely, there is, of course, the possibility that the Triassic and Tertiary intrusions are derived from partial melting of deep and unexposed Precambrian tin anomalies (Schuiling 1967), or that even a subcrustal tin anomaly is involved (Clark et al. 1976). A first regional study on the tin distribution in mid-Andean volcanic rocks by Lehmann and Pichler (1980) reported mean values of 2 ppm Sn in rhyolitic rocks of northern Chile and NW Argentina, 3 ppm Sn in rhyolitic rocks from the Bolivian Altiplano, and 4.5 ppm Sn in rhyolites and rhyodacites of the eastern Cordillera of central Bolivia (Los Frailes Formation). These data



Fig. 74. Location of sample groups discussed in text (stippled areas), and of major copper porphyry and tin ore deposits in the Central Andes

appear to define a positive regional tin gradient towards the Bolivian tin belt. This picture can be further accentuated by new data from Winkelmann (1983), Gardeweg et al. (1984), Ishihara et al. (1984), Tistl (1985), Lehmann (unpubl.) and Miller (1988).

Tin data on igneous rocks from the following areas in the greater region around the Bolivian tin belt are available (Fig. 74):

1. Granitic rocks from northern and central Chile (Antofagasta and Copiapó sections), subdivided into a Paleozoic and a Mesozoic-Cenozoic group; sample locations and petrographic and chemical data are given in Ishihara et al (1984). The samples of the Paleozoic group are dominantly biotite granites with initial Sr isotope ratios ≤ 0.706 (Shibata et al., 1984), and having a petrochemistry of partly S-type and partly I-type. The Mesozoic-Cenozoic group consists of a calcalkaline suite of predominantly quartz-monzodioritic to granodioritic composition and is associated with the famous Chilean copper porphyries. These granitoids are hornblende- and magnetite-bearing and have initial Sr isotope ratios around 0.704 (I-type; magnetite series) (Gustafson and Hunt 1975; Shibata et al. 1984).

2. The granitic rocks of the northern Bolivian tin belt are subalkaline and peraluminous biotite granodiorites (hornblende-bearing) to biotite-muscovite syenogranites. K-Ar age data define two granite populations: a Middle to Late Triassic group (225-202 Ma) and a Late Oligocene to Early Miocene group (28-19 Ma) (McBride et al. 1983). Both granite groups are locally associated with tin-tungsten deposits, and have been sampled - from north to south - in the Huato, Illampu, Zongo-Yani, Huayna Potosi, Chacaltaya, Unduavi, Taquesi and Chojlla intrusions, as well as in the Quimsa Cruz batholith (Lehmann 1979; Winkelmann 1983; Tistl 1985; Miller 1988). The Triassic granites in northern Bolivia are part of a 1200-km-long Permo-Triassic granite belt which extends to central Peru, and are interpreted as rift-associated intracratonic magmatism (Kontak et al. 1984). Initial Sr isotope data from southern Peru are in the range of 0.7081-0.7170 (Kontak et al. 1984), preliminary data from the Cordillera Real give 0.7079-0.7087 (McNutt and Clark 1983). The Zongo-Yani pluton is locally foliated and has a synkinematic metamorphic aureole attaining sillimanite grade (Bard et al. 1974). Recent Rb-Sr isotope data indicate a Permo-Carboniferous age (Harris 1988), and $\epsilon_{Nd}(T=284 \text{ Ma}) -6.0$ (Miller and Harris 1989). The Tertiary granites in northern Bolivia (Quimsa Cruz intrusions) are the more deeply eroded equivalents of the tin porphyry systems of central and southern Bolivia, with which they form an extended volcanoplutonic province related to the subduction of the Nazca plate under the South-American craton.

3. The Ordovician Cafayate and Cuchiyaco granites of the Pampean Ranges in northwestern Argentina are peraluminous, calcalkaline fractionation suites which range from biotite tonalite to biotite-muscovite granite (Rapela and

Shaw 1979; Rapela et al. 1982). These rocks have an initial Sr isotope ratio of 0.705; they are unmineralized (Saavedra et al. 1987).

4. The Cenozoic rhyolitic volcanism of the western Cordillera in the border area of Chile and Bolivia consists of ignimbrite sheets, subvolcanic stocks, lavas and tuffs of dacite to rhyolite composition with initial Sr isotope ratios of 0.705-0.713 and ϵ_{Nd} -4 to -8 (Klerkx et al. 1977; Hawkesworth et al. 1982; Hildreth and Moorbath 1988). The volcanic rocks belong to the magnetite series (Fe_2O_3/FeO mostly >2) and are locally associated with polymetallic, Au-bearing epithermal systems (Cabello 1986; Gardeweg et al. 1984).

5. Rhyodacitic ignimbrites and rhyolitic to dacitic lavas and tuffs from the Altiplano and eastern Cordillera of Bolivia have Upper Cenozoic age and cover the same Sr and Nd isotope compositional field as equivalent rocks from the Chile-Bolivia border area given above (Klerkx et al. 1977; Schneider 1985; Redwood 1986). Subvolcanic stocks and brecciated vents are associated with polymetallic hydrothermal systems. Erosion level controls the style of

mineralization, with tin-tungsten porphyry deposits at deeper levels (→ Llallagua) and epithermal precious metal-rich mineralization at shallow levels (Grant et al. 1977, 1980). Uranium deposits of roll-front type occur in the Altiplano (Michel and Schneider 1978).

Some geochemical data on the sample groups studied are compiled in Table 6. The Chilean rock samples were analyzed by atomic absorption spectrometry (detection limit: 0.2 ppm Sn), the remainder by X-ray fluorescence spectrometry (detection limit: 2-3 ppm Sn).

The tin data of the granitic samples are plotted in Figs. 75 and 76 as a function of Rb/Sr and TiO_2 . Two distribution patterns can be distinguished: (1) Positive or negative linear correlation for $\log[Sn]$ vs. $\log[Rb/Sr]$ or $\log[Sn]$ vs. TiO_2 (wt%), respectively; (2) no or weak correlation of Sn with the two indicators of fractionation, i.e. constantly low Sn content for a large interval of Rb/Sr and TiO_2 values. The two distribution patterns characterize the tin granite population from northern Bolivia and the non-tin granite population from Chile and NW Argentina, respectively. The correlation lines for the tin granite suite are statistically significant at the 99.9 % level of certainty, with

Table 6 (next two pages). Chemical parameters of sample groups from the Central Andes on which tin data are available (arithmetic means \pm 1 standard deviation). I and M means ilmenite- and magnetite-series rocks in the sense of Ishihara (1977)

Table 6 (continued)

Sample group	SiO ₂ (wt%)	Rb (ppm)	Sr (ppm)	TiO ₂ (wt%)	Rb/Sr	Sn (ppm)	Rock suite	References
<u>North-Central Chile granites</u> <u>(Antofagasta and Copiapo transects)</u>								
Biotite granites with SiO ₂ > 68 wt% (Late Paleozoic) (n = 16)	73.0 ±2.2	133 ±49	116 ±77	0.18 ±0.11	2.65 ±3.35	1.4 ±1.1	I/M	Ishihara et al. (1984) Shibata et al. (1984)
Biotite-hornblende granodiorites/ quartz monzonites (SiO ₂ < 68 wt%) (Mesozoic-Cenozoic) (n = 18)	62.5 ±3.6	84 ±46	466 ±155	0.60 ±0.20	0.19 ±0.12	1.4 ±0.6	M	Ishihara et al. (1984) Shibata et al. (1984)
<u>Northern Bolivian tin granites</u>								
Huato biotite granite (n = 9) (Triassic)	68.8 ±0.9	236 ±14	149 ±9	0.50 ±0.06	1.59 ±0.12	12 ±8	I	Tistl (1985)
Illampu biotite-hornblende grano- diorite (Triassic) (n = 9)	68.8 ±1.0	173 ±23	244 ±22	0.53 ±0.06	0.72 ±0.16	7 ±3	-	Miller (1988)
Zongo-Yani biotite-muscovite granite (Triassic) (n = 27)	73.2 ±1.4	374 ±137	86 ±62	0.20 ±0.11	5.91 ±3.59	21 ±11	I	Tistl (1985) Lehmann (1979)
Huayna Potosi biotite-muscovite granodiorite (Triassic) (n = 10)	69.1 ±2.9	215 ±95	210 ±95	0.47 ±0.22	2.50 ±3.21	13 ±12	I	Lehmann (1979)
Chacaltaya biotite-muscovite granite (Triassic) (n = 8)	71.3 ±2.3	448 ±140	56 ±24	0.22 ±0.12	11.4 ±10.2	29 ±9	I	Lehmann (1979)
Chacaltaya granite/greisen (tourma- line-muscovite alteration) (n = 16)	68.9 ±3.7	423 ±43	453 ±477	0.35 ±0.12	6.38 ±7.98	1112 ±2400	I	Lehmann (1979)
Unduavi biotite granodiorite (Triassic) (n = 10)	n.d.	177 ±20.3	366 ±20.9	0.599 ±0.047	0.488 ±0.070	4.9 ±2.0	I	Lehmann and Winkelmann (unpublished)
Taqesi biotite granodiorite/ granite (Triassic) (n = 12)	69.5 ±3.2	217 ±56	258 ±101	0.40 ±0.17	1.12 ±0.82	17 ±4	I	Winkelmann (1983)
Chojlla muscovite granite (n = 7)	73.4 ±2.7	744 ±88	20 ±7	0.03 ±0.02	44.7 ±20.2	242 ±145	I	Winkelmann (1983)
Quimsa Cruz biotite granodiorite/ granite (Tertiary) (n = 15)	68.6 ±3.7	303 ±93	352 ±251	0.53 ±0.21	2.13 ±3.10	13 ±10	-	Miller (1988)

Table 6 (continued)

Sample group	SiO ₂ (wt%)	Rb (ppm)	Sr (ppm)	TiO ₂ (wt%)	Rb/Sr	Sn (ppm)	Rock series	References
<u>Pampean Ranges granites, NW Argentina</u>								
Cafayate biotite granodiorite/tonalite (Ordovician) (n = 5)	64.1 ±2.6	79 ±25	275 ±54	0.46 ±0.14	0.32 ±0.15	<3.5	M	Rapela and Shaw (1979) Rapela et al. (1982)
Cafayate biotite-muscovite granite (Ordovician) (n = 18)	70.8 ±1.6	175 ±69	109 ±52	0.07 ±0.07	2.99 ±3.73	<3.5	I/M	Rapela and Shaw (1979) Rapela et al. (1982)
Cuchiyaco biotite-muscovite granodiorite (Ordovician) (n = 13)	69.0 ±1.2	95 ±10	151 ±26	0.14 ±0.05	0.65 ±0.20	<3.5	M	Rapela and Shaw (1979) Rapela et al. (1982)
<u>Western Cordillera rhyolites</u>								
Northern Chile and westernmost Bolivia (Cenozoic) (n = 39)	72.9 ±4.9	186 ±76	107 ±123	0.28 ±0.24	4.53 ±4.23	1.8 ±0.5	M	Klerkx et al. (1977) Pichler & Zell (1969, 1972)
<u>Guatiquina volcanic rocks, Chile</u>								
Rhyolitic rocks (> 68 wt% SiO ₂) (Tertiary) (n = 11)	70.2 ±2.2	182 ±26	237 ±76	n.d.	0.91 ±0.45	2.2 ±0.8	M	Gardeweg et al. (1984) Hawkesworth et al. (1982)
Andesitic rocks (< 68 wt% SiO ₂) (Tertiary) (n = 12)	62.5 ±3.0	139 ±24	352 ±108	n.d.	0.44 ±0.15	2.0 ±0.5	M	Gardeweg et al. (1984) Hawkesworth et al. (1982)
<u>Volcanic rocks of the Bolivian Altiplano</u>								
Southern Altiplano rhyodacites (Cenozoic) (n = 54)	65.3 ±9.5	170 ±62	281 ±79	0.65 ±0.17	0.66 ±0.38	3.0 ±0.5	M	Kusmaul et al. (1977) Fernandez et al. (1973)
Chorolque rhyodacite (tourmalinisericite alteration) (n = 22)	n.d.	276 ±57	147 ±116	0.62 ±0.03	4.77 ±7.61	75 ±139	-	Lehmann and Sanchez (unpublished)
Los Frailes Ignimbrite (rhyodacite) (Tertiary) (n = 19)	65.7 ±3.1	233 ±27	408 ±76	0.70 ±0.15	0.59 ±0.10	4.5 ±0.7	M	Michel (in preparation) Schneider (1985)
Northern Altiplano rhyodacites (Cenozoic) (n = 7)	66.6 ±1.7	132 ±21	711 ±213	0.66 ±0.09	0.20 ±0.05	<3.5	-	Redwood (1986)

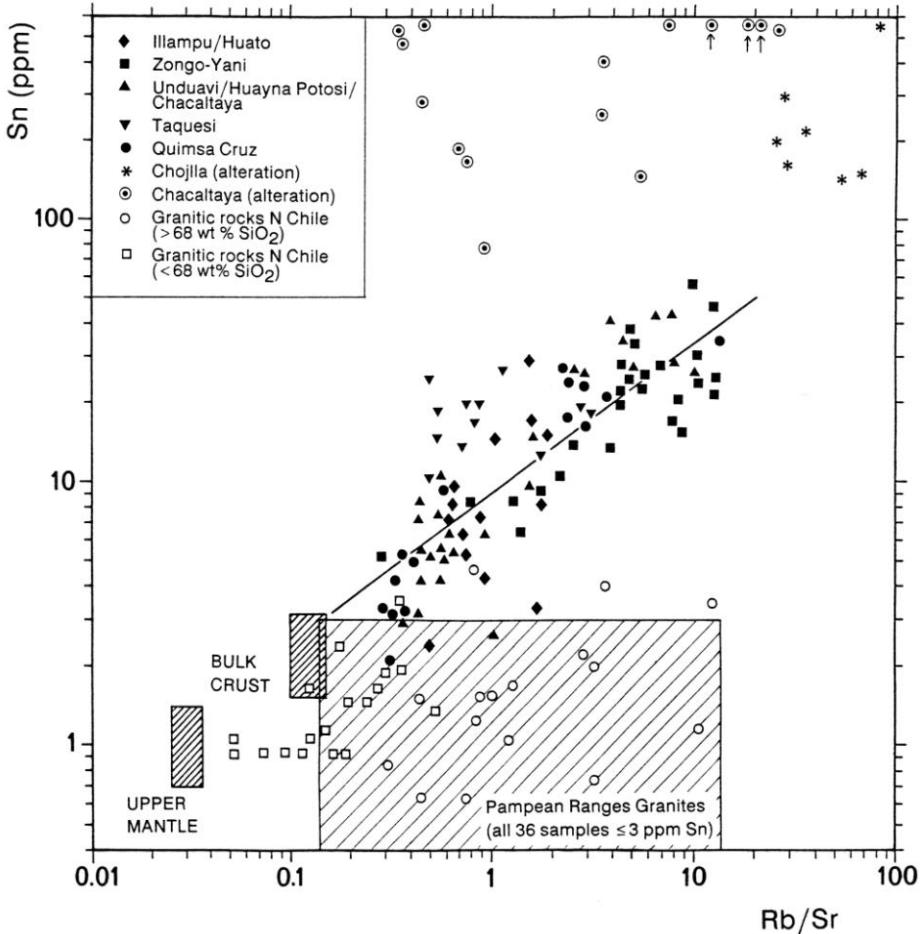


Fig. 75. Rb/Sr-Sn variation diagram for granitic rocks of the Central Andes. Tin granites of the northern Bolivian tin belt define a correlation line $\log[\text{Sn}] = 0.956 + 0.565 \log[\text{Rb}/\text{Sr}]$ with $r = 0.78$ ($n = 98$). Hydrothermally overprinted granite samples from the Chacaltaya and Chojlla tin ore systems give scatter distributions at high tin levels. Non-tin granites of northern Chile and NW Argentina (Pampean Ranges) have low tin contents and give no systematic tin enrichment trend during magmatic evolution. Bulk Crust and Upper Mantle reference fields according to Anderson (1983) and Taylor and McLennan (1985)

correlation coefficients of $r(\log \text{Rb}/\text{Sr} - \log \text{Sn})$ 0.78 and $r(\text{TiO}_2 - \log \text{Sn})$ 0.74 ($n = 98$). The geometric parameters of the correlation lines are very similar to those of tin granite suites in other parts of the world (Lehmann 1982).

Fractional crystallization is the dominant petrogenetic process which controls the magmatic evolution of both the Cordillera Real/Quimsa Cruz tin granites

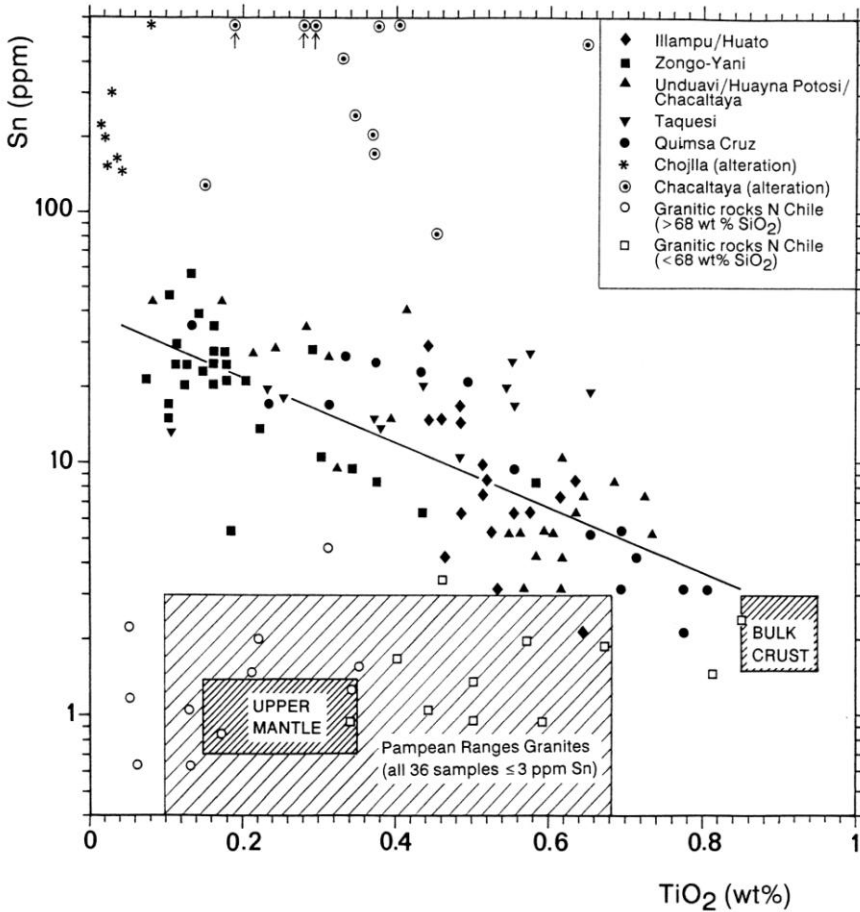


Fig. 76. TiO_2 -Sn variation diagram for granitic rocks of the Central Andes. Tin granites of the northern Bolivian tin belt define a correlation line $\log[\text{Sn}]=1.581-1.252[\text{TiO}_2]$ with $r=-0.74$ ($n=96$; hydrothermally overprinted sample populations from Chojlla and Chacaltaya mining areas are not included)

(Lehmann 1979, 1985) and the non-tin granites of NW Argentina (Rapela and Shaw 1979; Saavedra et al. 1987). The Rb-Sr plot in Fig. 77 underlines these earlier conclusions. Slope and length of the correlation trends point to the importance of plagioclase fractionation in both granite populations. The two different tin distribution patterns can therefore be interpreted to result from two different tin distribution coefficients, with $\bar{D}_{\text{Sn}}(\text{xtls/melt}) \approx 1$ in the non-tin granites and $\bar{D}_{\text{Sn}}(\text{xtls/melt}) < 1$ in the tin granites (Lehmann 1982). The correlation trends for the tin granite suite in Figs. 75 and 76 extend to the bulk-crust reference field, least evolved granite samples plot close to average

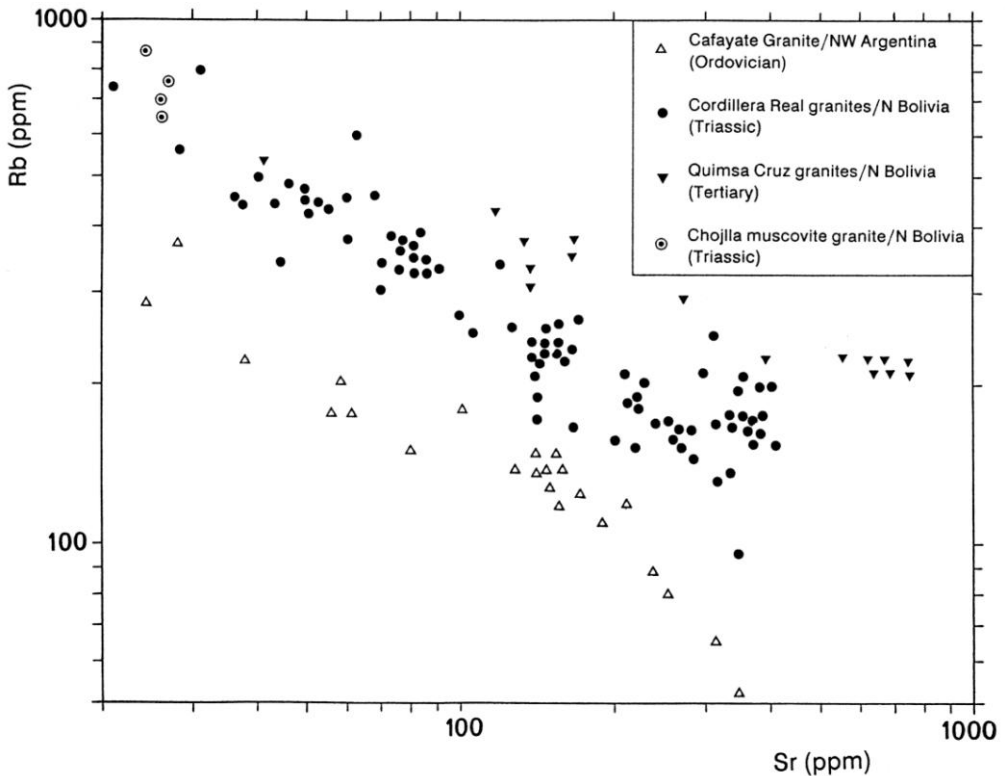


Fig. 77. Rb-Sr variation diagram for rock samples of the tin-barren Cafayate granite (Pampean Ranges, NW Argentina), the Cordillera Real tin granites, the Quimsa Cruz tin granites, and the muscovite granite of the Chojlla tin mine. Slope and extent of the linear correlation trends in log-log space suggest substantial plagioclase fractionation in all sample suites

crustal material. This situation points to an origin of the tin granites from a melt initially not anomalous in tin, and to source rocks of average crustal composition. A crustal source of the Bolivian tin granites is likely in view of their peraluminous S-type character (Clark and Robertson 1978; Lehmann 1979; Winkelmann 1983; Tistl 1985) and of their isotope characteristics (Kontak et al. 1984; McNutt and Clark 1983; Miller and Harris 1989).

The low initial Sr-isotope data of the granitic rocks from northern Chile and NW Argentina, on the other hand, suggest an important contribution by mantle material (Shibata et al. 1984; Rapela et al. 1982; Saavedra et al. 1987). Tin contents in these sample groups are very low (Chile: 1.4 ppm Sn; Argentina: all 36 samples analyzed <3.5 ppm Sn), in between average tin

contents for bulk crust and upper mantle. These non-tin granite suites are predominantly of magnetite-series affiliation with $\text{Fe}_2\text{O}_3/\text{FeO}$ ratios of >0.5 , distinctly different from the Bolivian ilmenite-series tin granites with $\text{Fe}_2\text{O}_3/\text{FeO}$ ratios of <0.1 (Lehmann unpubl.). Both $\text{Fe}^{3+}/\text{Fe}^{2+}$ ratio and opaque mineral assemblage reflect the oxygen fugacity during rock formation, which in magnetite-series granitic rocks is relatively high and favours the accessory mineral assemblage of magnetite-titanite (Ishihara 1981; see Chap. 2.4). Magnetite and titanite have exceptionally high tin distribution coefficients of $D_{\text{titanite}}(\text{xtl}/\text{melt}) \approx 60$ and $D_{\text{magnetite}}(\text{xtl}/\text{melt})$ 4-12 in granitic melts (Antipin et al. 1981), which may provide an explanation for the bulk tin distribution coefficient in magnetite-series rocks close to unity.

The hydrothermally overprinted granite samples of the Chacaltaya and Chojlla tin-tungsten mines in Bolivia give scatter patterns in Figs. 75 and 76. The Chacaltaya greisen samples are characterized by feldspar-destructive alteration and have the stable mineral assemblage quartz-muscovite-tourmaline-apatite-siderite-fluorite-cassiterite. The Chojlla apl granite has the stable assemblage quartz-oligoclase-microcline together with sub-solidus muscovite-tourmaline-apatite-cassiterite. Both the Chacaltaya and Chojlla samples show element distribution patterns established by fractional crystallization and enhanced and modified by fluid interaction.

The tin data of the volcanic rocks are plotted in Fig. 78 as a function of Rb/Sr. Titanium or zirconium contents are not very useful as indicators of fractionation in this rock group, which in the Bolivian sector has mostly $\text{SiO}_2 \leq 66$ wt%, because these components become less compatible towards intermediate melt composition and higher melt temperature, i.e. change their bulk distribution coefficients significantly.

The tin distribution pattern of the volcanic rocks is similar to the one in the granites: weak or no tin enrichment during magmatic evolution in barren volcanics, and distinct tin enrichment in samples from the Bolivian tin belt, where the least-evolved samples are near the bulk-crust reference field. The hydrothermally overprinted rhyodacitic rocks of the Chorolque tin porphyry system (tourmaline-sericite alteration) are characterized by high Rb/Sr ratios due to plagioclase destruction and Sr leaching. This fluid overprint is accompanied by tin enrichment up to subeconomic levels. There is a tendency to chemical continuum between magmatic and hydrothermal processes, which complicates the distinction between both stages.

Data for a classification of the Bolivian tin-bearing volcanics into ilmenite- or magnetite-series rocks are not sufficient and difficult to obtain in view of

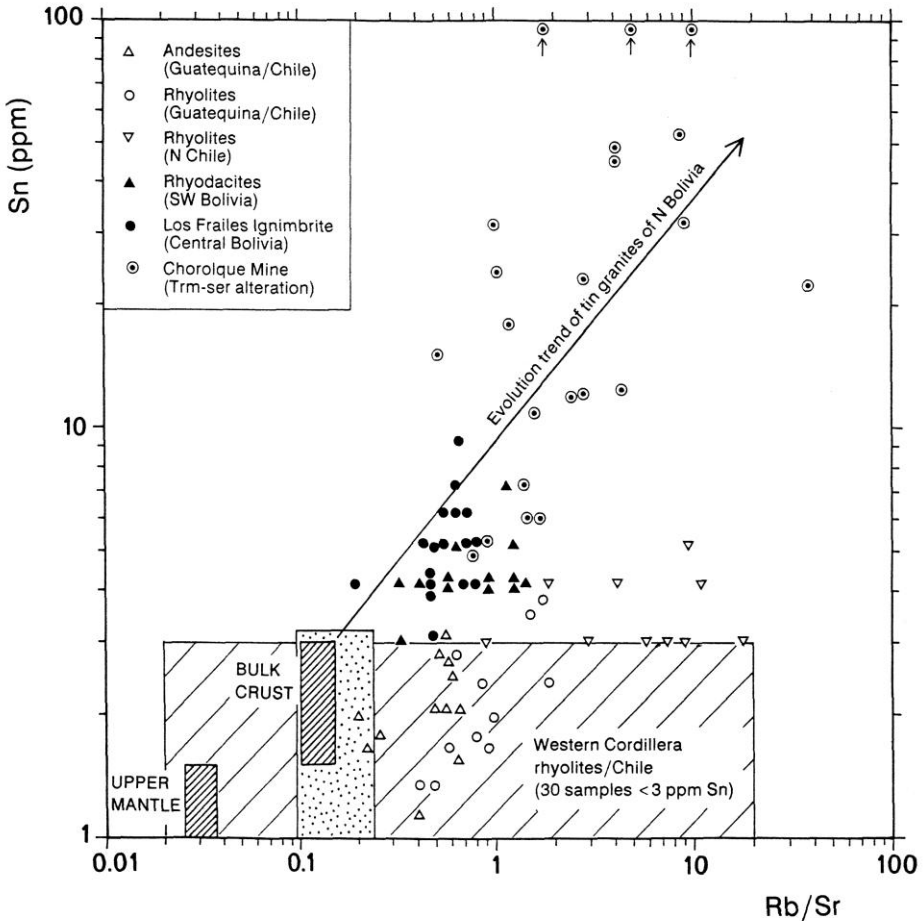


Fig. 78. Rb/Sr-Sn variation diagram for volcanic rocks of the Central Andes. The reference line gives the evolution trend of the tin granites of the northern Bolivian tin belt defined in Fig. 75. Rhyolitic rocks from the western Cordillera (Chile and westernmost Bolivia) have low tin contents and give no or very little tin enrichment during magmatic evolution. Rhyodacitic rocks from the Los Frailes Ignimbrite in Central Bolivia plot close to least-evolved tin granite samples of the Cordillera Real. Hydrothermally overprinted rocks from the Chorolque tin porphyry system give a scatter distribution at high tin levels. The stippled pattern enclosing the Bulk Crust reference field locates northern Altiplano rhyodacites (7 samples with ≤ 3 ppm Sn; Redwood 1986)

widespread alteration. Hydrothermal overprint and mineralization developed under conditions of relatively low oxygen fugacity in between the NNO and

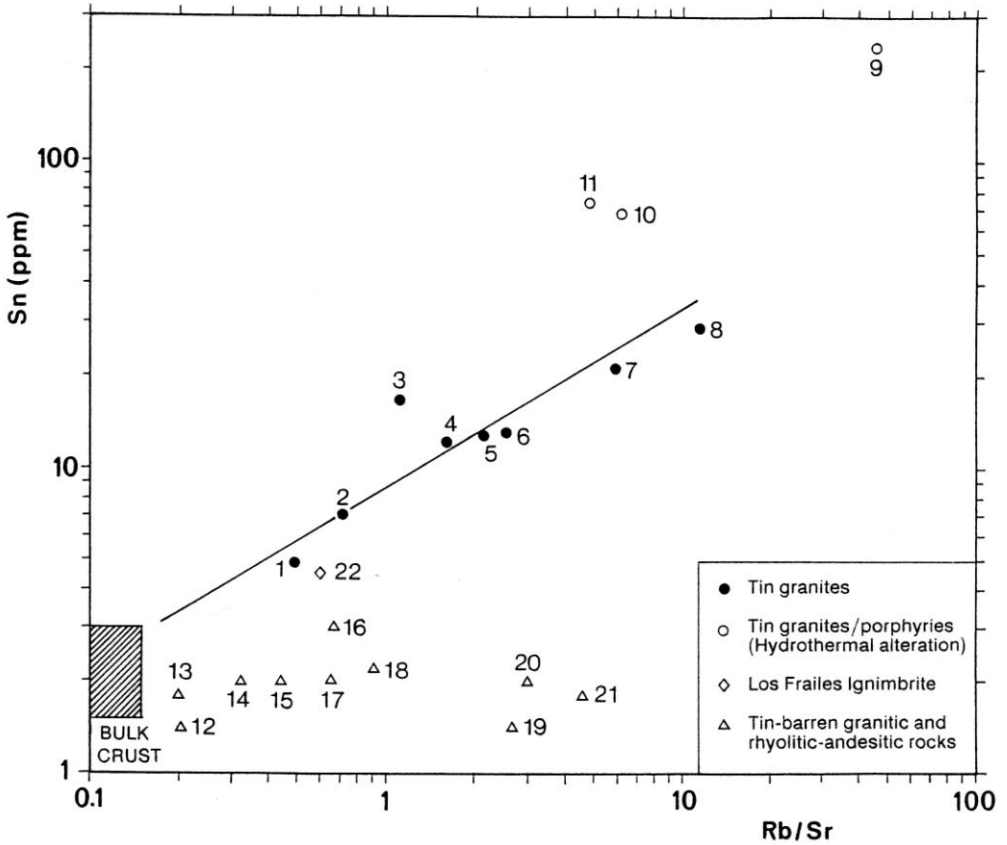


Fig. 79. Synoptic Rb/Sr-Sn variation diagram for arithmetic means of the sample populations studied. Tin-bearing granites define a tin enrichment trend as a function of degree of magmatic evolution. This trend extends back to average crustal rock composition. The Los Frailes ignimbrite from the periphery of the Central Bolivian tin belt plots close to the least-evolved part of this trend. Hydrothermally modified samples from tin ore systems have high tin levels, partly they are also most evolved magmatically (compare TiO_2 contents in Fig. 76 and Table 6). Tin barren granitic and rhyolitic rocks have low tin contents which do not correlate with degree of magmatic fractionation. 1 Unduavi granodiorite; 2 Illampu granodiorite; 3 Taquesi granodiorite/granite; 4 Huato granite; 5 Quimsa Cruz granites; 6 Huayna Potosi granite; 7 Zongo-Yani granite; 8 Chacaltaya granite; 9 Chojlla granite; 10 Chacaltaya greisen; 11 Chorolque rhyodacite; 12 N Chile grano-diorites; 13 Northern Altiplano rhyodacites; 14 Cafayate granodiorite; 15 Guatiquina andesites; 16 SW Bolivian rhyodacites; 17 Cuchiyaco granodiorite; 18 Guatiquina rhyolites; 19 N Chile granites; 20 Cafayate granite; 21 Western Cordillera rhyolites; 22 Los Frailes ignimbrite

QFM buffers (as inferred from the general paragenetic scheme of Kelly and Turneure 1970), with fluids in an early stage of magmatic origin (Grant et al. 1980). Given a rock-buffered fluid evolution an ilmenite-series affiliation of the volcanics seems probable. This contrasts with the rhyolites of the western Cordillera which belong to the magnetite series. The source material of both tin-bearing volcanics of the eastern Cordillera and tin-barren volcanics of the western Cordillera appears to be the lower crust (Sr and Nd isotope data by Klerkx et al. 1977; Hawkesworth et al. 1982; Schneider 1985; Redwood 1986; Hildreth and Moorbath 1988).

It is interesting to note that the Miocene-Pliocene Macusani ash-flow tuffs in SE Peru, about 60 km west of the San Rafael Sn-Cu deposit, have chemical characteristics very similar to the highly evolved portions of the tin granites of northern Bolivia. The Macusani volcanics have been studied by Noble et al. (1984) and Pichavant et al. (1987, 1988a,b) and have been discussed in petrogenetic terms of fractional crystallization and partial melting, the latter process being favoured by Pichavant et al. (1988b). The chemical data from Pichavant (1988b), thought to reflect the magmatic chemistry, give a range in tin content of 27-194 ppm (nine samples) with corresponding TiO_2 values of 0.22-0.04 wt%, and Rb/Sr of 3.4-710. These data would plot in the most evolved part of the correlation trends of Figs. 75 and 76. The highly fractionated nature of the Macusani volcanics is also displayed in systematic and characteristic enrichment and depletion patterns for other incompatible and compatible elements. These features, together with the ilmenite-series nature of the rocks (Noble et al. 1984; Pichavant et al. 1988a), identify the Macusani volcanic zone as a very promising area for tin mineralization in a porphyry environment.

In summary, it can be concluded that the geochemically better-defined Bolivian tin granites have systematic tin enrichment trends as a function of degree of fractionation. The non-tin granites from the periphery of the Bolivian tin belt show no analogous tin enrichment which can be understood as a consequence of an unfavourable bulk tin distribution coefficient near unity (magnetite-series granitic rocks). The least fractionated parts of the tin granite suite have tin contents typical of average crust, which does not support the assumption of anomalous tin contents in the source material of the Bolivian tin granites (Fig. 79).

5.4 Kelapa Kampit, Belitung Island, Indonesia

The Kelapa Kampit tin deposit on Belitung Island is the economically most important example of strata-bound tin mineralization in the SE Asian tin belt. It has often been cited as an example of synsedimentary precursor mineralization later remobilized during granite magmatism, and is therefore of great importance in a general metallogenic context. Kelapa Kampit is also a key locality for the concept of lithophile-element mineralization associated with mafic volcanism, which was first put forward for tungsten by Maucher (1965) and later extended to tin mineralization by Plimer (1980). The genetic interpretation of an ore deposit is in this concept primarily based on geometric parameters which have been emphasized by Amstutz (1959:12): "Congruency may be used as an indication of syngenetic origin". This claim invites confusion between the phenomenology and nature of an ore deposit, because hydrothermal fluid circulation and ore deposition are controlled by the permeability structure of the enclosing medium, which in turn depends on lithological parameters. Inherent lithological contrasts will result in variable degree of stratabound fluid flow at a scale defined by the local geology.

The Kelapa Kampit Mine is today focussed on open-pit bulk mining of the Nam Salu horizon. Earlier selective mining of a large cassiterite-sulphide vein system (bedding-plane lodes and discordant veins) has been abandoned. The Nam Salu horizon is a steeply dipping, 15-40-m- thick, iron-rich phyllite which consists of laminated pyrrhotite-pyrite-magnetite in a matrix of stilpnomelane-biotite-chlorite, with some actinolite-rich calcsilicate lenses. Cassiterite occurs in fine-grained disseminations (average grain size around 50 μ) over a strike length of 3 km at a geochemical level of 200 ppm Sn, and in the Nam Salu open pit over a length of about 100 m reaches an economic grade of 1-1.5 wt% Sn (Greg Bolton, PT Preussag, pers. commun. 1985). The Nam Salu horizon is part of a Permo-Carboniferous low-grade rock sequence which consists of predominantly clastic sediments with intercalations of limestone, chert, and ironstone associated with submarine mafic volcanism (Adam 1960; Osberger 1962). The sequence is intruded by Triassic granites which are tin-bearing (see Tanjungpandan Pluton; Chap. 4.1). Igneous rocks in the immediate Kelapa Kampit area are however restricted to rare porphyry dikes; larger granite outcrops are 20 km away.

The Nam Salu ore horizon has relic tuff fabrics and was identified by Schwartz and Surjono (1986) as metasomatically altered, tuffitic banded iron formation. The tin-mineralized rock portions have high contents of Rb, Cs, Be, Pb, Bi, W and Zn; a feature distinctly different from sea-water overprinted meta-basalts

Table 7. Arithmetic means of some element contents in major rock units of the Kelapa Kampit mining area, Indonesia. Data from Schwartz and Surjono (1986), meta-basalt reference data from Lehmann (1988b).

	1	2	3	4	5	6	7
SiO ₂	34.23	32.49	53.68	82.19	90.33	46.03	48.20
TiO ₂	1.08	1.46	1.21	0.35	0.14	0.72	3.27
Al ₂ O ₃	9.62	11.61	12.80	6.36	3.25	6.36	12.95
Fe ₂ O ₃	39.87	40.72	19.42	5.26	2.66	27.12	14.42
MnO	0.38	2.14	0.37	0.15	0.10	0.66	0.18
MgO	3.64	3.20	3.36	1.16	0.81	3.28	5.55
CaO	0.13	0.43	1.00	0.02	0.01	11.62	8.83
Na ₂ O	0.07	0.09	0.57	0.16	0.13	0.28	2.07
K ₂ O	4.16	2.33	2.28	1.37	0.79	0.31	0.68
P ₂ O ₅	0.10	0.09	0.12	0.03	0.02	0.10	0.40
L.O.I.	3.77	3.83	3.46	2.10	1.18	2.34	3.05
Total	97.05	98.38	98.28	99.16	99.40	98.81	99.60
n	23	7	5	19	2	3	6
Ba	403	370	114	178	123	152	18
Bi	163	<6	<6	<6	<6	<6	<6
Ce	69	80	81	62	37	37	96
Cr	116	115	86	43	76	46	74
Cs	325	-	-	-	-	-	-
Cu	169	17	31	32	36	198	114
F	603	-	-	-	-	-	542
La	155	133	70	34	13	37	176
Nb	52	13	12	7	5	11	13
Ni	41	41	41	17	13	91	28
Pb	216	4960	3000	1200	447	<5	<5
Rb	1380	577	317	129	81	39	19
Sc	13	22	19	5	4	16	31
Sn	16400	90	42	127	135	434	<3
Sr	13	20	54	8	4	100	201
Ta	<5	<5	<5	<5	<5	<5	<5
Th	30	26	24	24	21	16	12
U	13	6	4	3	<3	6	4
V	152	215	151	83	26	116	295
W	115	12	21	9	<5	<5	<5
Y	89	33	33	18	7	24	44
Zn	354	3630	5030	1050	293	788	115
Zr	78	106	32	152	30	63	204

- 1 = Nam Salu horizon in open pit (stilpnomelane-biotite-chlorite-magnetite-pyrrhotite-pyrite phyllite)
 2 = Nam Salu horizon in exploration drilling (core samples)
 3 = Country rock of Nam Salu horizon (chlorite schist)
 4 = Country rock of Nam Salu horizon (meta-siltstone)
 5 = Country rock of Nam Salu horizon (chert)
 6 = Country rock of Nam Salu horizon (calcsilicate rock)
 7 = Meta-basalt (spilite), 35 km NW of Kelapa Kampit

n = number of samples analyzed. Fe₂O₃ is total iron.

(spilites) from the same sequence several kilometers away, which have Cr, Ni and V levels similar to the Nam Salu horizon without, however, any lithophile element enrichments (Table 7). The high Rb and Cs contents of the Nam Salu horizon argue against a sea water-dominated hydrothermal system. The mineralogical-geochemical character of the mineralization suggests a granite-related situation in the sense of sulphide replacement, with the reactive material consisting of mafic tuff which is petrochemically very close to dolomitic carbonate material. The potassic alteration style and the crystal morphology of the Nam Salu cassiterite (short prismatic habitus) point to relatively high temperature of the hydrothermal overprint/mineralization (Omer-Cooper et al. 1974; Ahlfeld 1931; Kelly and Turneaure 1970; Rutherford 1969).

The conventional model which infers a metal source by means of an unexposed tin granite has yet to be positively proven by drilling or radiometric dating of the mineralizing event. There is the analogous case of the Sangdong scheelite deposit in Korea which was resolved recently. The Sangdong strata-bound tungsten mineralization in Cambrian limestones indicated, through its mineralogical, geochemical and stable isotope zoning pattern, a granitic intrusion at depth. Recent drilling revealed 500 m beneath the main orebody the expected Upper Cretaceous highly evolved granite (Moon 1988, 1989).